

Modern Physics Letters A
 © World Scientific Publishing Company

NEUTRON STAR SEQUENCES AND THE STARQUAKE GLITCH MODEL FOR THE CRAB AND THE VELA PULSAR

P. S. Negi

Department of Physics, Kumaun University, Nainital - 263002, India
psnegi_nainital@yahoo.com; negi@aries.ernet.in

Received (Day Month Year)

Revised (Day Month Year)

We construct for the first time, the sequences of stable neutron star (NS) models capable of explaining simultaneously, the glitch healing parameters, Q , of both the pulsars, the Crab ($Q \geq 0.7$) and the Vela ($Q \leq 0.2$), on the basis of starquake mechanism of glitch generation. These models yield an upper bound on surface redshift of NSs, $z_R \simeq 0.77$. If the lower limit of the observational constraint of (i) $Q \geq 0.7$ for the Crab pulsar and (ii) the recent value of the moment of inertia for the Crab pulsar (evaluated on the basis of time-dependent acceleration model of the Crab Nebula), $I_{\text{Crab},45} \geq 1.93$ (where $I_{45} = I/10^{45} \text{ g.cm}^2$), both are imposed together on these models, the models yield the value of matching density, $E_b = 9.584 \times 10^{14} \text{ g cm}^{-3}$ at the core-envelope boundary. This value of matching density yields a model-independent upper bound on neutron star masses, $M_{\text{max}} \leq 2.22M_\odot$, and the strong lower bounds on surface redshift $z_R \simeq 0.6232$ and mass $M \simeq 2.11M_\odot$ for the Crab ($Q \simeq 0.7$) and the strong upper bound on surface redshift $z_R \simeq 0.2016$, mass $M \simeq 0.982M_\odot$ and the moment of inertia $I_{\text{Vela},45} \simeq 0.587$ for the Vela ($Q \simeq 0.2$) pulsar. However, for the observational constraint of the ‘central’ weighted mean value $Q \approx 0.72$, and $I_{\text{Crab},45} > 1.93$, for the Crab pulsar, the minimum surface redshift and mass of the Crab pulsar are slightly increased to the values $z_R \simeq 0.655$ and $M \simeq 2.149M_\odot$ respectively, whereas corresponding to the ‘central’ weighted mean value $Q \approx 0.12$ for the Vela pulsar, the maximum surface redshift, mass and the moment of inertia for the Vela pulsar are slightly decreased to the values $z_R \simeq 0.1645$, $M \simeq 0.828M_\odot$ and $I_{\text{Vela},45} \simeq 0.459$ respectively. These results set an upper and lower bound on the energy of a gravitationally redshifted electron-positron annihilation line in the range of about 0.309 - 0.315 MeV from the Crab and in the range of about 0.425 - 0.439 MeV from the Vela pulsar.

Keywords: Dense matter; Equation of state; Stars-neutron.

PACS Nos.: 04.20.Jd; 04.40.Dg; 97.60.Jd.

1. Introduction

The data on the glitch healing parameter, Q , provide the best tool for testing the starquake (Ruderman 1972; Alpar et al 1996) and Vortex unpinning (Alpar et al 1993) models of glitch generation in pulsars. Both of these mechanisms of glitch generation, in fact, consider NSs, in general, a two component structure: a superfluid interior core surrounded by a rigid crust (in the present study we shall

use the term ‘envelope’ which includes the solid crust and other interior portion of the star right up to the superfluid core). In the starquake model, Q is defined as the fractional moment of inertia, i.e. the ratio of the moment of inertia of the superfluid core, I_{core} , to the moment of inertia of the entire configuration, I_{total} , as (Pines et al 1974)

$$Q = \frac{I_{\text{core}}}{I_{\text{total}}}. \quad (1)$$

Recently, Crawford & Demiański (2003) have collected the all measured values of the glitch healing parameter Q for Crab and Vela pulsars available in the literature and found that for 21 measured values of Q for Crab glitches, a weighted mean of the values yields $Q = 0.72 \pm 0.05$, and the range of $Q \geq 0.7$ encompasses the observed distribution for the Crab pulsar. In order to test the starquake model for the Crab pulsar, they have computed Q (as given by Eq.(1)) values for seven representative equations of state (EOSs) of dense nuclear matter, covering a range of neutron star masses. Their study shows that the much larger values of $Q (\geq 0.7)$ for the Crab pulsar is fulfilled by all the six EOSs (out of seven considered in the study) corresponding to a ‘realistic’ neutron star mass range $1.4 \pm 0.2 M_{\odot}$. By contrast, a weighted mean value of the 11 measurements for Vela yields a much smaller value of $Q (= 0.12 \pm 0.07)$ and the all estimates for Vela agree with the likely range of $Q \leq 0.2$. Thus, their results are found to be consistent with the starquake model predictions for the Crab pulsar. They have also concluded that the much smaller values of $Q \leq 0.2$ for the Vela pulsar are inconsistent with the starquake model predictions, since the implied Vela mass based upon their models corresponds to a value $\leq 0.5 M_{\odot}$ for $Q \leq 0.2$, which is too low as compared to the ‘realistic’ NS mass range.

Thus, in the literature, the starquake is considered as a viable mechanism for glitch generation in the Crab and the vortex unpinning, the another mechanism, is considered suitable for the Vela pulsar, since it can avoid some other problems associated with the starquake explanation of the Vela glitches (see, e.g. Crawford & Demiański (2003); and references therein). However, it seems surprising that if the internal structure of NSs are described by the same two component conventional models (as mentioned above), different kinds of glitch mechanisms are required for the explanation of a glitch! Furthermore, it also follows from the above discussion that the main reason for not considering the starquake, the feasible mechanism for glitch generation in the Vela, lies in the fact that there exists none of the sequence of NS models in the literature which could explain simultaneously, on the basis of starquake model, both the extreme limiting cases of glitch healing parameter, Q , corresponding to the Vela ($Q \leq 0.2$) and the Crab ($Q \geq 0.7$) pulsars in the range $0 \leq Q \leq 1.0$ for the ‘realistic’ NS mass values for both the pulsars. The present study, therefore, deals with the construction of such models ^a

^ahowever, the other problems associated with the starquake explanation of the Vela glitches (see,

We assume that *all* the NSs belong to the same family of NS sequence which terminates at the *maximum* value of mass. Certainly, this *maxima* should correspond to an *upper bound* on NS masses. In order to construct such a sequence, we have to set the extreme causal EOS (in geometrized units), $dP/dE = 1$ (where P is the pressure and E the energy-density) to describe the core. Firstly, because various observational studies like - the gamma-ray burst data, X-ray burst data and the glitch data etc., and their explanation (see, e.g. Lindblom 1984; Cottam et al 2002; Datta & Alpar 1993) favour the stiffest EOSs. The latest estimate of the moment of inertia for the Crab pulsar (based upon the ‘newest’ observational data on the Crab nebula mass) rules out most of the existing EOSs of the dense nuclear matter, leaving only the stiffest ones (Bejger & Haensel 2002; Haensel et al 2006). Secondly, because of the fact that the ‘real’ EOS of the dense nuclear matter beyond the density range $\sim 10^{14} \text{ g cm}^{-3}$ are largely unknown due to the lack of knowledge of nuclear interactions (see, e.g. Dolan 1992; and references therein; Haensel et al 2006), and the various EOSs available in the literature (see, e.g. Arnett & Bowers 1977) for NS matter represent only an extrapolation of the results far beyond this density range. Though, the status of the ‘real’ EOS for NS matter is not certain, one could impose some well-known physical principle, independent of the EOS, such as the ‘causality condition’ ($dP/dE = 1$) throughout the core of the star beyond a fiduciary density, E_b , at the core-envelope boundary to ascertain a definite upper bound on NS masses (see, e.g., Rhoades & Ruffini 1974; Hartle 1978; Lindblom 1984; Friedman & Ipser 1987; Kalogera & Baym 1996). In this connection this is also to be pointed out here that the maximum mass for *any* EOS describing the core, beyond the density E_b , with a subluminal sound velocity turns out to be less than that of the upper bound obtained by using the extreme causal EOS (see, e.g., Haensel et al 2006).

The envelope of our models (below the density E_b at the core-envelope boundary) may be characterized by the well-known EOS of classical polytrope $\text{dln}P/\text{dln}\rho = \Gamma_1$ (where ρ denotes the density of the rest-mass and Γ_1 is a constant known as the adiabatic index) for different values of the constant $\Gamma_1 = (4/3), (5/3)$ and 2 respectively. The reason for considering the polytropic EOS for the entire envelope lies in the fact that with this EOS, our models yield an upper bound on NS masses *independent* of the value of Γ_1 , and this upper bound (for a fiduciary choice of E_b) is found fully consistent with those of the values cited in the literature (Kalogera & Baym 1996; Friedman & Ipser 1987). Thus, the choice of the said polytropic EOS for the entire envelope may be regarded entirely equivalent to the choice of the various EOSs like WFF (Wiringa, Fiks & Fabrocini 1988), FPS (Lorenz, Ravenhall & Pethick, 1993), NV (Negele & Vautherin 1973), or BPS (Baym, Pethick & Sutherland 1971) in an appropriate sequence below the density range E_b , adopted

e.g. Crawford & Demiański (2003); and references therein) are not considered in the present paper. The future study in this regard may provide some explanation, provided the correlation between various parameters of the Crab and the Vela pulsar, obtained in the present study, can be utilized.

by various authors in the conventional models of NSs (see, e.g., Kalogera & Baym 1996; Friedman & Ipser 1987), so that the constant Γ_1 appearing in the polytropic EOS may be looked upon as an ‘average’ Γ_1 for the density range below E_b , specified by the sequence of various EOSs in the conventional models of NSs. The choice of the constant $\Gamma_1 = 4/3, 5/3$ and 2 thus become obvious, since this choice can cover almost the entire range of density discussed in the literature for NS matter which is also applicable for the envelope region - the polytropic EOS with $\Gamma_1 = 4/3$ represents the EOS of extreme relativistic degenerate electrons and non-relativistic nuclei (Chandrasekhar 1935), $\Gamma_1 = (5/3)$ represents the well-known EOS of non-relativistic degenerate ‘neutron gas’ (Oppenheimer & Volkoff 1939), and $\Gamma_1 = 2$ represents the case of extreme relativistic baryons interacting through a vector meson field (Zeldovich 1962) (The value of $\Gamma_1 > 2$ is also possible for some EOS describing the NS matter, e.g., Malone, Johnson & Bethe 1975; Clark, Heintzmann & Grewing 1971, however, the results obtained in this paper remain unaffected for the choice of $\Gamma_1 > 2$), and the outcome of this study (in terms of explaining the glitch healing parameter for various pulsars and predicting the upper bound on the compactness of NSs (since the upper bound on mass is independent of the value of Γ_1)) would finally decide, among the chosen values, the ‘appropriate’ value of Γ_1 for the NS envelope. The validity of assuming the extreme causal EOS in the core and a polytropic EOS in the envelope of the present models, in view of the various modern EOS of dense nuclear matter, is also discussed in the last section of the present paper.

We have noted that in all conservative models of NSs, the choice of the core-envelope boundary, r_b (corresponding to a density denoted by E_b), is somewhat *arbitrary* in the sense that there are no criteria available for the choice of a particular matching density, E_b , below which the EOS of the NS matter is assumed to be known and unique. One can freely choose somewhat lower values of E_b (which will increase the core size) to obtain higher values of Q (see, e.g. Shapiro & Teukolsky 1983; Datta & Alpar 1993). To avoid such a procedure, we choose the core-envelope boundary of our models on the basis of the ‘compatibility criterion’ which asserts that for an assigned value of the ratio (σ) of central pressure, P_0 , to central energy-density, E_0 , the compactness parameter $u(\equiv M/R$; total mass to radius ratio) of any *regular* configuration should not exceed the compactness parameter u_h of the homogeneous density sphere, in order to assure the compatibility with the hydrostatic equilibrium (Negi & Durgapal 2001; Negi 2004a). This criterion is capable of constraining the core-envelope boundary of any physically realistic NS model. A combination of this criterion with those of the observational data on the glitch healing parameter and the recently estimated minimum value of the moment of inertia for the Crab pulsar (based on the newly estimated ‘central value’ of the Crab nebula mass $M(\text{nebula}) \simeq 4.6M_\odot$ in the time-dependent acceleration model), $I_{\text{Crab},45} = 1.93$; where $I_{\text{Crab},45} = I_{\text{Crab}}/10^{45} \text{ g cm}^2$ (Bejger & Haensel 2003) can provide the desired NS models discussed above, since both the theory (criterion)

and the observations (stated above) are being used to construct the NS models.

2. Methodology

The metric for spherically symmetric and static configurations can be written in the following form

$$ds^2 = e^\nu dt^2 - e^\lambda dr^2 - r^2 d\theta^2 - r^2 \sin^2 \theta d\phi^2, \quad (2)$$

where ν and λ are functions of r alone. The Oppenheimer-Volkoff (O-V) equations (Oppenheimer & Volkoff 1939), resulting from the Einstein field equations for systems with isotropic pressure P and energy-density E can be written as

$$P' = -(P + E)[4\pi Pr^3 + m]/r(r - 2m) \quad (3)$$

$$\nu'/2 = -P'/(P + E) \quad (4)$$

$$m'(r) = 4\pi Er^2; \quad (5)$$

where the prime denotes the radial derivative and $m(r)$ represents the mass contained within the radius r

$$m(r) = \int_0^r 4\pi Er^2 dr.$$

The coupled Eqs.(3 - 5), are solved for the model (supplemented by the boundary conditions: $P = E = 0$, $m(r = R) = M$, $e^\nu = e^{-\lambda} = (1 - 2M/R) = (1 - 2u)$ at $r = R$) by considering the EOS, $dP/dE = 1$, in the core and choosing various values of Γ_1 in the polytropic envelope for various assigned values of σ such that for each value of σ , the compactness ratio of the whole configuration always turns out to be less than or equal to the compactness ratio of the corresponding sphere (with the same σ) of the homogeneous density distribution and should not exceed the *exact* absolute upper bound on compactness ratio of NSs compatible with causality and pulsational stability (see, e.g. Negi 2004b). We find that this condition is uniquely fulfilled by all models corresponding to an envelope with $\Gamma_1 = (4/3), (5/3)$ and 2 respectively, if the *minimum* value of the ratio of pressure to energy-density, P_b/E_b , at the core-envelope boundary reaches about 4.694×10^{-2} . The results of the study are presented in Fig.1 for the value of matching density, $E_b = 9.584 \times 10^{14} \text{ g cm}^{-3}$, i.e. about 3.55 times the nuclear saturation density (note that the particular choice of E_b used here turns out to be a consequence of the constraints (i) and (ii) mentioned in the abstract of the present study, and therefore, does not represent a fiduciary quantity as discussed in the next section). It is seen that the models become pulsationally stable up to the maximum value of mass $M_{\text{max}} \simeq 2.22M_\odot$ and radius, $R \simeq 9.64 - 10.81 \text{ km}$. The minimum radius results for the model with a $\Gamma_1 = 2$ envelope thus maximizes the compactness ratio for the stable configuration, $u \simeq 0.34$, as shown in Table 1. This behaviour indicates that among various values of Γ_1 chosen in the envelope for the density range right from 3.55 times the nuclear saturation density

(P_0/E_0)	u_h	u^a	u^b	u^c
0.06927	0.10813	0.04176	0.08454	0.09544
0.08411	0.12531	0.04959	0.09679	0.10925
0.10786	0.14970	0.06679	0.11761	0.13131
0.12029	0.16116	0.07693	0.12843	0.14236
0.13005	0.16960	0.08509	0.13671	0.15077
0.13357	0.17253	0.08804	0.13966	0.15370
0.14549	0.18205	0.09798	0.14940	0.16340
0.15354	0.18814	0.10461	0.15572	0.16969
0.20061	0.21911	0.14077	0.18919	0.20255
0.23990	0.24008	0.16698	0.21268	0.22536
0.27901	0.25763	0.18963	0.23274	0.24469
0.34816	0.28259	0.22255	0.26156	0.27253
0.44840	0.30929	0.25816	0.29256	0.30222
0.48306	0.31666	0.26795	0.30094	0.31024
0.51773	0.32332	0.27667	0.30848	0.31746
0.63150	0.34115	0.29895	0.32778	0.33589
0.66866	0.34593	0.30438	0.33242	0.34040
0.68296	0.34766	0.30623	0.33404	0.34194
0.69900	0.34952	0.30820	0.33573	0.34352
0.72302	0.35220	0.31076	0.33793	0.34567
0.74010	0.35401	0.31235	0.33934	0.34700
0.77503	0.35751	0.31501	0.34164	0.34914
0.80605	0.36041	0.31656	0.34294	0.35044
0.83972	0.36336	0.31711	0.34347	0.35091

up to zero at the surface, the ‘average’ value of Γ_1 is appropriately described by a polytropic index $n = 1$. This fact will also follow from some special features of the model with $\Gamma_1 = 2$ envelope discussed in the next section. The binding energy per unit mass $\alpha[\equiv (M_r - M)/M]$; where M_r is the rest-mass (see, e.g. Shapiro & Teukolsky 1983)] also approaches a maximum for about 0.3201 for the maximum value of mass up to which the configurations remain pulsationally stable. However, for the $\Gamma_1 = (4/3)$ envelope model the binding energy reaches a maximum beyond the maximum value of mass.

3. An application of the models to the Crab and Vela pulsars

For slowly rotating configurations like the Crab and Vela pulsars (rotation velocity about 188 and 70 rad sec⁻¹ respectively) the moment of inertia may be calculated in the first order approximation that appears in the form of the Lense-Thirring frame dragging-effect. For Crab and Vela pulsars, the first-order effects turn out to be about 1 - 2% (other effects like mass shift and deformation from spherical

symmetry due to rotation represent second-order effects which are significant for the case of millisecond pulsars. For Crab and Vela like pulsars, the second-order effects turn out to be about 10^{-4} or even lower; see, e.g. Arnett & Bowers 1977; Crawford & Demiański 2003. Therefore, these effects can be safely ignored when studying the macroscopic parameters of the slowly rotating pulsars as carried out in the present paper). These effects are reproduced by an empirical formula that is based on the numerical results obtained for thirty theoretical EOSs of dense nuclear matter. For NSs, the formula yields (Bejger & Haensel 2002)

$$I \simeq \frac{2}{9}(1 + 5x)MR^2, \quad x > 0.1 \quad (6)$$

where x is the compactness ratio measured in units of $(M_{\odot}(\text{km})/\text{km})$, i.e.

$$x = \frac{M/R}{M_{\odot}/\text{km}} = \frac{u}{1.477} \quad (7)$$

only static (non-rotating) parameters of the spherical configuration appear in the formula.

Equation (6) is used, together with coupled Eqs.(3 - 5), to calculate the fractional moment of inertia given by Eq.(1) and the moment of inertia of the entire configuration for an assigned value of the matching density, E_b . It is seen that among all models corresponding to different values of Γ_1 in the envelope, the lower limits of both the observational constraints for the Crab pulsar, $Q \geq 0.7$ and $I_{\text{Crab},45} \equiv I_{\text{total},45} \geq 1.93$, are appropriately satisfied by the $\Gamma_1 = 2$ envelope model. Since this particular model yields a unique value of matching density, $E_b = 9.584 \times 10^{14} \text{ g cm}^{-3}$, for the last two constraints in such a manner that the constraint $I_{\text{total},45} \geq 1.93$ is appropriately fulfilled by all stable NS models corresponding to the $\Gamma_1 = (5/3)$ and 2 envelopes for another constraint $Q \geq 0.7$ as shown in Figs.2 and 3 respectively (the model with a $\Gamma_1 = (4/3)$ envelope is ruled out since it always yields stable models with $Q < 0.7$). Another special feature of the $\Gamma_1 = 2$ envelope model lies in the fact that it yields somewhat wider range of glitch healing parameter, $0 < Q \leq 0.78$, for the stable models as compared to the $\Gamma_1 = (5/3)$ envelope model which yields this parameter in the range $0 < Q \leq 0.75$ for stable models as shown in Fig.2. Furthermore, the $\Gamma_1 = 2$ envelope model yields somewhat higher value of maximum surface redshift, $z_R \simeq 0.2016$, for the Vela pulsar ($Q \simeq 0.2$) and somewhat lower value of minimum surface redshift, $z_R \simeq 0.6232$, for the Crab pulsar ($Q \simeq 0.7$) simultaneously, as compared to the $\Gamma_1 = (5/3)$ envelope model. Thus provides somewhat wider range of lower and upper bounds on the energy of a gravitationally redshifted radiation from the surface of the Vela and the Crab pulsars respectively. And above all, the compactness maximizes, $u \simeq 0.34$, for the $\Gamma_1 = 2$ envelope model in the stable sequence of NS models as shown in Fig.1. This special feature of the model is also discussed in section 2.

The above-mentioned features indicate the appropriateness of the $\Gamma_1 = 2$ envelope model and thus emerges an important consequence of this study which states

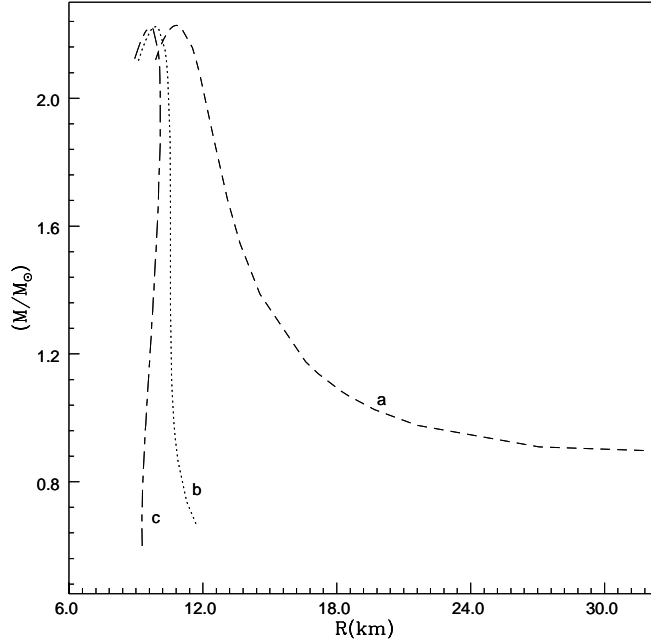


Fig. 1. Mass-Radius diagram of the models as discussed in the text for the value of matching density $E = E_b = 9.584 \times 10^{14} \text{ g cm}^{-3}$ at the core-envelope boundary. The labels a, b and c represent the models for an envelope with $\Gamma_1 = (4/3), (5/3)$ and 2 respectively. The minimum value of the ratio of pressure to energy-density, (P_b/E_b) , at the core envelope boundary is obtained as 4.694×10^{-2} , such that for an assigned value of σ , the inequality $u \leq u_h$ is always satisfied for *all* the models as shown in Table 1.

that the envelope of ‘real’ NSs may be well approximated by an EOS of classical polytrope with ‘average’ value of polytropic index, n , closer to 1.

For the minimum value of $Q \simeq 0.7$, Fig.3 yields $I_{\text{total},45} \equiv I_{\text{Crab},45} \simeq 1.93$ for the $\Gamma_1 = 2$ envelope model and by the use of Fig.2 and Table 1, we obtain the minimum values of mass, $M \simeq 2.11M_\odot$, and surface redshift, $z_R \simeq 0.6232$, for the Crab pulsar. On the other hand, for the maximum value of $Q \simeq 0.2$ which belongs to the Vela pulsar, Fig.3 yields $I_{\text{total},45} \simeq 0.587$ corresponding to the $\Gamma_1 = 2$ envelope model and Fig.2 and Table 1 yield the maximum values of mass, $M \simeq 0.982M_\odot$, and surface redshift, $z_R \simeq 0.2016$, for the Vela pulsar (note that the upper weighted mean value of $Q \approx 0.19$ for the Vela pulsar, Fig.2 and Table 1 (for the $\Gamma_1 = 2$ envelope model) yield the maximum value of mass, $M \simeq 0.961M_\odot$, and surface redshift, $z_R \simeq 0.1966$, for the Vela pulsar. Obviously, these values are much closer to the values corresponding to the maximum value of $Q \approx 0.2$ for the Vela pulsar). However, for the observational constraint of the ‘central’ weighted mean values of $Q \approx 0.72$ for the Crab and $Q \approx 0.12$ for the Vela pulsar, Fig.2 and Table

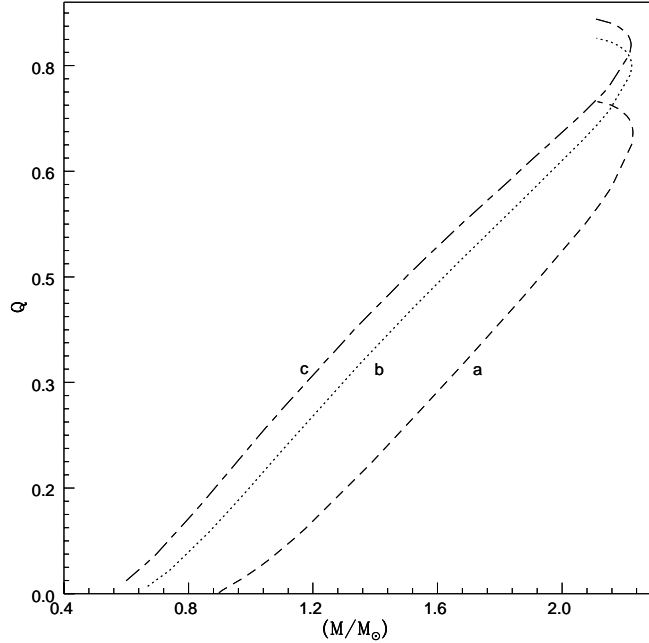


Fig. 2. Fractional moment of inertia $Q(\equiv I_{\text{core}}/I_{\text{total}})$ vs. total mass M for the configurations presented in Fig.1. The labels a, b and c represent the models for an envelope with $\Gamma_1 = (4/3), (5/3)$ and 2 respectively.

1 (for the $\Gamma_1 = 2$ envelope model) yield the slightly increased values of mass, $M \simeq 2.149M_\odot$, and the surface redshift, $z_R \simeq 0.655$, for the Crab and somewhat decreased values of mass, $M \simeq 0.828M_\odot$, and surface redshift, $z_R \simeq 0.1645$, for the Vela pulsar respectively. For these central weighted mean values of Q , Fig.3 yields for the $\Gamma_1 = 2$ envelope model, the moment of inertia $I_{\text{Crab},45} \simeq 1.971$ for the Crab and $I_{\text{Vela},45} \simeq 0.459$ for the Vela pulsar respectively. For the lower weighted mean value of $Q \approx 0.05$ corresponding to the Vela pulsar, Fig.2 and Table 1 yield (for the $\Gamma_1 = 2$ envelope model) the minimum values of mass, $M \simeq 0.685M_\odot$, and surface redshift, $z_R \simeq 0.1312$, whereas Fig.3 yields a minimum value of moment of inertia, $I_{\text{Vela},45} \simeq 0.355$, for the Vela pulsar.

4. Implications of the models for the extraordinary gamma-ray burst GRB790305b

Apart from the models of the Crab and Vela pulsars, let us consider two of the main findings related to the extraordinary gamma-ray burst of 5 March 1979: (i) it gives

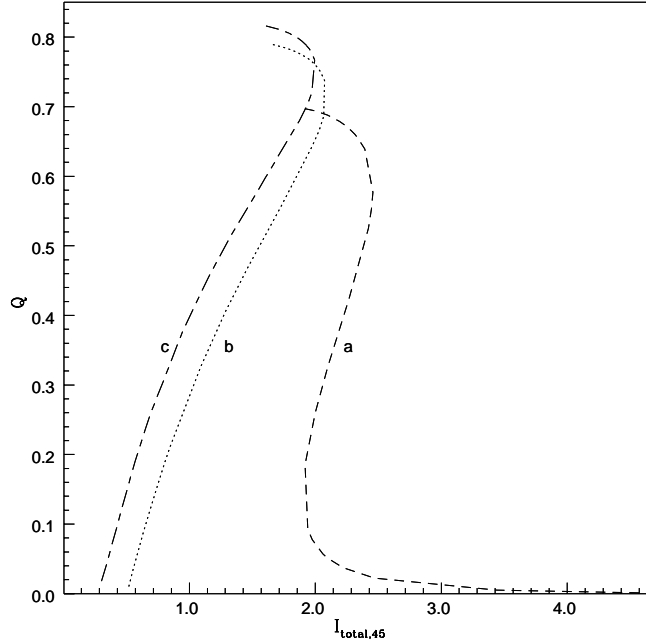


Fig. 3. Fractional moment of inertia $Q(\equiv I_{\text{core}}/I_{\text{total}})$ vs. moment of inertia of the whole structure $I_{\text{total},45}$ for the configurations presented in Fig.1. The labels a, b and c represent the models for an envelope with $\Gamma_1 = (4/3), (5/3)$ and 2 respectively. $I_{\text{total},45}$ is defined as $I_{\text{total}}/10^{45} \text{ g cm}^2$.

the only reliable estimate of the surface redshift, $z_R = 0.23 \pm 0.07$ (after taking due account of thermal blueshift), associated with the supernova remnant N49 in the Large Magellanic Cloud (see, e.g. Higdon & Lingenfelder 1990; Douchin & Haensel 2001; and references therein), and (ii) the implied peak luminosities of the repeating burst GRB790305b correspond to an energy of 10^{44} ergs, which is possible only when a starquake releases at least 10^{-9} of the NS gravitational binding-energy of 10^{53} ergs (Higdon & Lingenfelder 1990). In order to reproduce both of these findings, one would require a NS model compatible with starquake model predictions that could also account for a surface redshift $z_R = 0.23 \pm 0.07$. Both of these requirements are, in fact, fulfilled by our models. For the case of the $\Gamma_1 = 2$ envelope model, we get from Fig.2 - 3 the central value of surface redshift $z_R = 0.23$ for a mass $M \simeq 1.095 M_\odot$ with $Q \simeq 0.259$. The binding energy corresponding to this case is obtained as 2.618×10^{53} ergs which is capable of releasing 2.618×10^{44} ergs of energy required for the latter burst.

5. Results and conclusions

This study constructs the stable sequences of NS models terminate at the value of maximum mass, $M_{\max} \simeq 2.22M_{\odot}$, independent of the EOSs of the envelope, for the matching density, $E_b = 9.584 \times 10^{14} \text{ g cm}^{-3}$, at the core-envelope boundary. This value of ‘matching density’ is a consequence of the observational constraints $Q \simeq 0.7$ and $I_{\text{Crab},45} \simeq 1.93$ (associated with the Crab pulsar) imposed together on the $\Gamma_1 = 2$ envelope model and in this sense does not represent a fiduciary quantity. The upper bound of the surface redshift, $z_R \simeq 0.77$ (corresponding to a u value $\simeq 0.34$), however, belongs to the model with a $\Gamma_1 = 2$ envelope which is consistent with the absolute upper bound on the surface redshift of NS models compatible with causality and pulsational stability (Negi 2004b). This special feature, together with some other remarkable ones, discussed in the present study underline the appropriateness of the $\Gamma_1 = 2$ envelope model.

Since among the variety of modern EOSs discussed in the literature, the upper bound on NS mass compatible with causality and dynamical stability can reach a value up to $2.2M_{\odot}$ (in this category, the SLy (Douchin & Haensel 2001) EOS yields a maximum mass of $2.05M_{\odot}$, whereas the BGN1 (Balberg & Gal 1997) and the APR (Akmal et. al. 1998) EOSs yield the maximum masses of $2.18M_{\odot}$ and $2.21M_{\odot}$ respectively (see, e.g. Haensel et al 2006)). In view of this result, the model-independent maximum mass, $M_{\max} \simeq 2.22M_{\odot}$, obtained in this study may be regarded as good as those obtained on the basis of modern nuclear theory.

In addition to this result, the appropriate sequences of stable NS models obtained in this study can explain the glitch healing parameter, Q , of any glitching pulsar, provided the weighted mean values of Q lie in the range $0 < Q \leq 0.78$. This finding also reveals that if the starquake is considered to be a viable mechanism for glitch generation in all pulsars, then the envelope of ‘real’ NSs may be well approximated by a polytropic EOS corresponding to a polytropic index, n , closer to 1.

For the value of matching density, $E_b = 9.584 \times 10^{14} \text{ g cm}^{-3}$, the $\Gamma_1 = 2$ envelope model yields the minimum values of mass $M \simeq 2.11M_{\odot}$ and surface redshift $z_R \simeq 0.6232$ for the Crab ($Q \simeq 0.7$) and the maximum values of mass $M \simeq 0.982M_{\odot}$ and surface redshift $z_R \simeq 0.2016$ for the Vela pulsar ($Q \simeq 0.2$). The minimum mass and surface redshift for the Crab pulsar are slightly increased up to the values $M \simeq 2.149M_{\odot}$ and $z_R \simeq 0.655$ respectively, if the ‘central’ weighted mean value of $Q \approx 0.72$ and the moment of inertia $I_{\text{Crab},45} > 1.93$ are also imposed on these models. However, for the ‘central’ weighted mean value of $Q \simeq 0.12$ corresponding to the Vela pulsar, the maximum mass and surface redshift are somewhat decreased to the values $M \simeq 0.828M_{\odot}$ and $z_R \simeq 0.1645$ respectively. This value of mass and surface redshift for the Vela pulsar can further decrease up to the values $M \simeq 0.685M_{\odot}$ and $z_R \simeq 0.1312$ respectively, if the lower weighted mean value of $Q \simeq 0.05$ for the Vela pulsar is imposed. These results predict the upper and lower bounds on the energy of a gravitationally redshifted electron-positron annihilation line in the range of about 0.309 - 0.315 MeV from the Crab and in the range of about 0.425 -

0.439 MeV from the Vela pulsar respectively.

For a comparison, if the observational constraint of the minimum value of $I_{\text{Crab},45} \simeq 3.04$ (the value of moment of inertia for the Crab pulsar obtained earlier by Bejger & Haensel (2002), on the basis of the constant-acceleration model for the Crab nebula) together with $Q \simeq 0.7$ is imposed on the models studied in the present paper, the $\Gamma_1 = 2$ envelope model yields the value of matching density, $E_b = 7.0794 \times 10^{14} \text{ g cm}^{-3}$. This value of E_b yields a model-independent upper bound on NS mass $M_{\text{max}} \simeq 2.59M_{\odot}$. This value of maximum mass, however, represents an ‘average’ of the maximum NS masses in the range $2.2M_{\odot} \leq M_{\text{max}} \leq 2.9M_{\odot}$ obtained by Kalogera & Baym 1996 (and references therein) on the basis of other EOSs for NS matter, fitted to experimental nucleon-nucleon scattering data and the properties of light nuclei. For this lower value of matching density, the $\Gamma_1 = 2$ envelope models yield the minimum value of mass $M \simeq 2.455M_{\odot}$ for the Crab ($Q \simeq 0.7$) and the maximum value of mass $M \simeq 1.142M_{\odot}$ for the Vela pulsar ($Q \simeq 0.2$). The minimum mass for the Crab pulsar is slightly increased up to the value $M \simeq 2.5M_{\odot}$, if the ‘central’ weighted mean value of $Q \approx 0.72$ and the moment of inertia $I_{\text{Crab},45} > 3.04$ are also imposed on these models. However, corresponding to the ‘central’ weighted mean value of $Q \simeq 0.12$, the maximum mass of the Vela pulsar is somewhat decreased to the value $M \simeq 0.964M_{\odot}$. This value of mass for the Vela pulsar can further decrease up to the value $M \simeq 0.796M_{\odot}$, if the lower weighted mean value of $Q \simeq 0.05$ for the Vela pulsar is imposed.

Furthermore, the study can also explain some special features associated with the extraordinary gamma-ray burst of 5 March 1979.

Acknowledgments

The author acknowledges the Aryabhata Research Institute of Observational Sciences (ARIES), Nainital for providing library and computer-centre facilities.

References

1. Akmal, A., Pandharipande, V. R., & Ravenhall, D. G., 1998, Phys. Rev. C 58, 1804 (APR)
2. Alpar, M. A., Chau, H. F., Cheng, K. S., & Pines, D. 1993, ApJ 409, 345
3. Alpar, M. A., Chau, H. F., Cheng, K. S., & Pines, D. 1996, ApJ 459, 706
4. Arnett, W. D., & Bowers, R. L. 1977, ApJS 33, 415
5. Balberg, S., & Gal A., 1997, Nucl. Phys. A 625, 435 (BGN1)
6. Baym, G., Pethick, C., & Sutherland, P. 1971, ApJ, 170, 299 (BPS)
7. Bejger, M., & Haensel, P. 2002, A&A 396, 917
8. Bejger, M., & Haensel, P. 2003, A&A 405, 747
9. Chandrasekhar, S. 1935, MNRAS, 95, 207
10. Clark, J. W. Heintzmann, H., & Grewing, M. 1971, Astrophys. Letters 10, 21
11. Cottam, J., Paerels, F., & Mendez, M. 2002, Nature 420, 51
12. Crawford, F., & Demiański, M. 2003, ApJ 595, 1052
13. Datta, B., & Alpar, M. A. 1993, A&A 275, 210
14. Dolan, J. F. 1992, ApJ 384, 249

15. Douchin, F., & Haensel, P. 2001, A&A 380, 151 (SLy)
16. Friedman, J. L., & Ipser, J. R. 1987, ApJ 314, 594
17. Haensel, P., Potekhin, A. Y., & Yakovlev, D. G. 2006, Neutron Stars 1. Equation of State and Structure, Springer
18. Hartle, J. B. 1978, Phys. Rep. 46, 201
19. Higdon, J. M., & Lingenfelder, R. E., 1990, ARA&A 28, 401
20. Kalogera, V. & Baym, G. 1996, ApJ 470, L61
21. Lindblom, L. 1984, ApJ 278, 364
22. Lorenz, C. P., Ravenhall, D. G., & Pethick, C. J. 1993, Phys. Rev. Lett. 70, 379 (FPS)
23. Malone, R. C., Johnson, M. B., & Bethe, H. A. 1975, ApJ 199, 741
24. Negi, P. S., & Durgapal, M. C. 2001a, Grav. & Cosmol. 7, 37 (astro-ph/0312516)
25. Negi, P. S. 2004a, Mod. Phys. Lett. A 19, 2941 (astro-ph/0210018)
26. Negi, P. S. 2004b, Int. J. Mod. Phys. D. 13, 157 (astro-ph/0403492)
27. Negele, J., & Vautherin, D. 1973, Nucl. Phys., A207, 298 (NV)
28. Oppenheimer, J. R., & Volkoff G. M. 1939, Phys. Rev. 55, 374
29. Pines, D., Shaham, J., & Ruderman, M. 1974, IAU Symp. 53. Physics of Dense Matter, ed. C. J. Hansen (Dordrecht: Reidel), 189
30. Rhoades, C. E. Jr., Ruffini, R. 1974, Phys. Rev. Lett. 32, 324
31. Ruderman, M. 1976, ApJ, 203, 213
32. Shapiro, S. L., & Teukolsky, S. A. 1983, Black Holes, White Dwarfs, and Neutron Stars: The Physics of Compact Objects (New York: Wiley)
33. Wiringa, R. B., Fiks, V., & Fabrocini, A. 1988, Phys. Rev. C 38, 1010
34. Zeldovich, Ya. B. 1962, Soviet Phys., JETP, 15, 1158